EFFECT OF HUBBARD POTENTIAL ON STRUCTURAL AND ELECTRONIC PROPERTIES OF Mn SUBSTITUTED $CdIn_2Te_4$ CHALCOPYRITE SEMICONDUCTOR

PH-591

submitted by

SWAGATIKA MAHAPATRA
411PH2099

Under the guidance of

DR. BIPLAB GANGULI

DEPARTMENT OF PHYSICS
NATIONAL INSTITUTE OF TECHNOLOGY
ROURKELA

Declaration

I do hereby declare that the research work incorporated in the thesis entitled ”EFFECT OF HUBBARD POTENTIAL ON STRUCTURAL AND ELECCTRONIC PROPERTIES OF Mn SUBSTITUTED $CdIn_2Te_4$ CHALCOPYRITE SEMICONDUCTOR” is an original research work carried out by us in the Department of Physics, NIT Rourkela, under the supervision and guidance of Dr.Biplab Ganguli.

Date: (Swagatika Mahapatra)

DEPARTMENT OF PHYSICS

NIT, ROURKELA

CERTIFICATE

This is to certify that the project thesis entitled, “EFFECT OF HUBBARD POTENTIAL ON STRUCTURAL AND ELECTRONIC PROPERTIES OF Mn SUBSTITUTED $CdIn_2Te_4$ CHALCOPYRITE SEMICONDUCTOR” which is being submitted by Swagatika Mahapatra, M.Sc. student of Department of Physics, National Institute of Technology, Rourkela in partial fulfillment of the requirements for the degree of M.Sc. in Physics is carried out under my guidance.

(Dr. Biplab Ganguli)

ACKNOWLEDGEMENT

I heartily express my deepest sense of gratitude to my supervisor Dr. Biplab Ganguli, NIT Rourkela for his suggestion and guidance .His great interest, encouragement and guidance had made my work fruitful.

I express my special thanks to the research scholars, Computational Physics Lab for their valuable suggestions and guidance throughout my dissertion work.

Date: (Swagatika Mahapatra)

ABSTRACT

Chalcopyrite semiconductor consists of two zinc blende structure one above the other and have the general formula ABC_2. The Chalcopyrite semiconductors can be found in three different configurations such as pure form (ABC_2), defect form (AB_2C_4) and doped form (ABC_2D_4). Structural and electronic properties of CuFeSe2 and CdMnIn2Te4 are carried out using plane wave and pseudo potential method included in the QUANTUM ESPRESSO. Hubbard U parameter is calculated using linear response approach taking the extrapolation of U_{out} vs. U_{in}. The structural parameters such as the lattice parameter 'a', `c', tetragonal distortion (η) and anion displacement (u_x,u_y,u_z) are calculated using the energy minimization procedure. The total density of states, spin resolved density of states and band structure are calculated to carry out the electronic properties. A comparison is made on the structural and electronic properties using the Hubbard correction.

Contents

1 Introduction

The chalcopyrite semiconductor have general formula ABC_2. A,B,C are the atoms. It is a zinc blende superstructure, that is, it is the ternary analogus of the zinc blende. The Bravais lattice of the chalcopyrite is body centered tetragonal. The tetragonal unit cell of a typical chalcopyrite semiconductor consists of two zinc blende unit cells and can be obtained by doubling the zinc blende structure along the z-axis and filling the lattice sites[1]. Every atom is bonded to four first neighbour in a tetrahedral structure. Chalcopyrite compounds are of two types $A^I B^{III} C_2^{VI}$ and $A^{II} B^{IV} C_2^V$ such that the roman letters represents the group number in the periodic table. $A^I B^{III} C_2^{VI}$ and $A^{II} B^{IV} C_2^V$ are ternary analogous of the zinc blende type binary compounds $A^{II} B^{VI}$ and $A^{III} B^V$ respectively. There are four group I/II atoms, four group III/IV atoms and eight group VI/V atoms per unit cell of the pure chalcopyrite type semiconductor [1].

The chalcopyrite semiconductors can be found in three different configurations such as pure form (ABC_2), defect form (AB_2C_4) and doped form (ABC_2D_4). In defect chalcopyrite, there are vacancies in the compounds, that is, the group I/II element are missing and replaced by an empty sphere. If we dope a suitable atom in tha vacant space of defect chacopyrite such that the periodicity is maintained, then it is called doped chalcopyrite. The

crystal structure is same for both defect and doped chalcopyrite.

These semiconductors have received attention recently for their application in nonlinear optical devices, detectors, solar cells, light emitting diode, photo voltaic cells, and also useful for nonlinear optical frequency conversion and optoelectronic applications [1].

2 Computational Methods

Structural and electronic properties of $CuFeSe_2$ and $CdMnIn_2Te_4$ are studied by using density functional theory, plane wave method and atomic pseudopotentials [2] included in the QUANTUM ESPRESSO[3]. ESPRESSO stands for opEn Source Package for Research in Electronic Structure, Simulation and Optimization. Text input files in Quantum espresso are based upon fortran-95 in Quantum Espresso. Fortran-95 shows high performance and also it is a advanced programming technique. Using periodic boundary conditions, the codes are constructed. For any crystal structure, metal or insulator Quantum Espresso can be used. Hubbard U correction, local density calculation can be done using Quantum ESPRESSO.

In Quantum ESPRESSO, the self consistent solution of the Kohn Sham equation(KS) is found. The Kohn Sham equation is given by,

$$\left(\frac{-\hbar^2}{2m}\nabla^2 + V_{ext}(r) + V^{in}(r)\right)\psi_i(r) = \epsilon_i\psi_i(r) \tag{1}$$

where, ϵ_i and ψ_i are KS energy and orbitals respectively, i labels the occupied states, V_{ext} is the sum of the pseudopotentials of atomic cores, the input Hartree and exchange-correlation potential is a functional of the input charge density ρ_{in}.

The structure of $CuFeSe_2$ and $CdMnIn_2Te_4$ are generated using the Xcrysden tool [4]. The bond lengths and bond angles are also calculated

using this tool.

The Hubbard U parameter is calculated using the linear response approach [5], in terms of density response function of the system with respect to the localized perturbations. The effective interaction parameter U is calculated from the difference of the bare and screened second derivative of energy with respect to onsite occupations as given by,

$$U = \frac{\partial^2 E[\lambda_1]}{\partial {\lambda_1}^2} - \frac{\partial^2 E^{ks}[\lambda_1]}{\partial \lambda_1^2} = (X_0^{-1} - X^{-1}) \tag{2}$$

where, λ_1 represent the on-site occupation. Kulik et.al. [6] have argued that U should be consistently obtained from the GGA+U ground state itself. U_{scf} represents the effective on-site electron-electron interaction already present in the GGA energy functional for the GGA+U ground state when U is chosen to be U_{in}. Consistency is enforced by choosing U_{in} to be equal to U_{scf}. Taking the second derivative of the E, U_{out} is found as,

$$U_{out} = U_{scf} - \frac{U_{in}}{m}, m = \frac{1}{\sum_i (a_i^I)^2} \tag{3}$$

Here m is the effective degeneracy of the orbital whose population is changing during the perturbation. Thus, from linear response calculations for different U_{in} ground states we are able to extract the U_{scf}.

3 Literature Survey

3.1 $CuFeSe_2$

N Hamdadou et.al.[7] have grown $CuFeSe_2$ thin films by selenization of $CuFe$ alloy precursor. It is seen that the films exhibit (112) preferential orientation. These films are composed of well faceted grains and the thickness of the grains is of the same order of magnitude as that of the $CuFeSe_2$ films. Cu-rich films are n-type with a room temperature resisytivity of $(5-9)x10^2$ ohm cm, while fe-rich films are p-type with a room temperature resistivity of $(3-5)x10^1$ohm cm.

According P. C. Lee et. al. [8], $CuFeSe_2$ which is a member of $I-III-VI_2$ semiconductors, shows different physical property from the chacopyrite family including tetragonal structure. Its band gap is 0.16ev and it shows weak magnetic behaviour. A $CuFeSe_2$ thin film with thickness 200nm on SiO_2/Si substrate was prepared by pulse laser deposition. The temperature dependence of thermal conductivity and seeback coefficient were measured in a wide range of temperature from 150-300K. The room temperature thermal conductivity and seeback coefficient are obtained to be 3.5 w/m-K and -108v/K respectively.

A. I. Najafov et. al. [9] have found that the two polytypes of $CuFeSe_2$ tetragonal structure exist. P-type lattice with p_{42c} space group and param-

eters a = 5.50 , c = 11.00 is obtained by GTR method. The alternative valences of Cu and Fe atoms for Bridgman growth method causes nonstoichiometry of crystals.

Yu-Kuei Hsu et. al. [10] successfully synthesized the ternary semiconducting $CuFeSe_2$ nanocrystals of aq particular shape and size. Elemental analysis yield an atomic ratio of Cu:Fe:Se of 1 : 1.06 : 2.17. Bandgap is found to be 0.16 eV. Tetragonal phase is found and lattice constants a=5.53 and c=11.05 . XRD analysis confirmed the phase transformation with the reaction temperature. The SEM images showed the evolution of the resulting phase and shape of $CuFeSe_2$ NPs from irregular to cuboid. The mechanism of the formation rectangular solid ternary $CuFeSe_2$ NPs is determined by the reaction temperature.

J. M. Delgado et. al. [11] have reported that the crystal structure of $CuFeSe_2$ is tetragonal, with a = 5.530 , c = 11.049 . The structure is a superstructure based upon a cubic close packed array of anions with the cations occupying a fraction of the available tetrahedral sites.

J.lamazares et. al. [12] have studied of the magnetic, transport and mossbauer properties of $CuFeSe_2$. It shows significant differences from that of its homologous sulfide, chacopyrite($CuFeS_2$). Going down to 77k from room temperature, $CuFeSe_2$ is paramagnetic and metallic with a non-magnetic Mossbauer spectrum showing two equally populated sites for iron with very

small quadrupole splitting. It gives a tetragonal structure giving cell parameters of a = 5.539 , c = 11.060 , c/a=2.0.

A. M. Polubotko et. al. [13] pointed out the charge transfer in the $CuFeSe_2$ compound in paramagnetic region has a ferron type of transport with ferrons of a small radius. For some another specimen the charge transfor may be carried out by ferrons of a large radius at very low temperatures. The result are well confirmed by the temperature dependence of resistivity and by metal type of the compound.

$CuFeSe_2$ which is chalcopyrite type semiconductor shows different properties compared to chalcopyrite semiconductor ($CuFeS_2$). The detail theoretical work is not done in this system. This system can be applied for Hubbard correction. So this system is chosen for the study.

3.2 $CdMnIn_2Te_4$

Wanqi Jie et. al.[14] grown $CdMnIn_2Te_4$ by Bridgman method with x=0.1, 0.22 and 0.4. Several regions phases are crystallized. The magnetic susceptibility of phase is measured showing the result of antiferromagnetic interactions between Mn^{2+} ions. Large grain size was obtained from phase region. For x=0.4 rotation angle is positive with small value and negative for x=0.1 and 0.22.

Yongqin Chang et. al.[15] taken ACRT-B method to grow $Mn_xCd_{1-x}In_2Te_4$ with x=0.1. Here the composition distribution and growth interface profile shape were analyzed. In alpha phase growth process the partition ratio of solutes Mn, Cd & In are 1.286, 1.926 and 0.729 and in beta phase growth process they are found to be 1.120, 1.055 and 0.985. When In increases along the longitudinal axis Mn and Cd contents decrease and increase when In decrease with the distance from the centerline of ingot.

Chang Yong Qin et. al.[16] have grown $Mn_xCd_{1-x}In_2Te_4$ by Bridgman method with x=0.1, 0.22 and 0.4. At the tip of $Mn_xCd_{1-x}In_2Te_4$, $\alpha+\beta+\beta 1$ structures are formed. When temperature is below solidius, $\beta 1$ is precipitated from α phase and with the growth process, β phase increases.

F.palacio et.al.[17] have worked in the temperature range between 1.8 and 300k. The magnetic behaviour of $Mn_xCd_{1-x}In_2Te_4$ has been investigated

with 0.07$\leq$ x $\leq$1.0. When x=1. 0.90, 0.62 the freezing temperature has been found to be T_f= 3.9, 3.5 and 2.2k respectively. When x=0.22 and 0.07 the sample behave as paramagnet.

4 Results and Discussion

4.1 $CuFeSe_2$

The plane wave cutoff energy(ecut) is found using the total energy vs ecut diagram as shown in figure 1. As the total energy get saturated at 20 Ry so ecut is taken to be 20Ry.

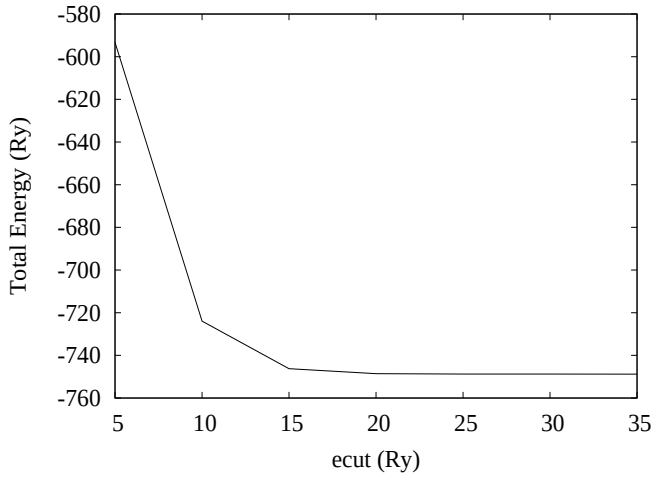

Figure 1: Total energy vs ecut for $CuFeSe_2$

Figure 2 shows the unit cell of $CuFeSe_2$ chalcopyrite semiconductors. The positions of the various atoms in the tetragonal unit cell of $CuFeSe_2$ are: Cu (0,0,0), Fe (0,0,0.5) and Se (0.25, 0.25, 0.125). For an ideal chalcopyrite structure, the tetragonal distortion, η=c/2a = 1. But if it is not ideal then the Se position is (u_x, u_y, u_z) where u_x, u_y and u_z are anion displacement parameters along three axes. In this case, the Se atoms displace from ideal

position. This is called as anion displacement.

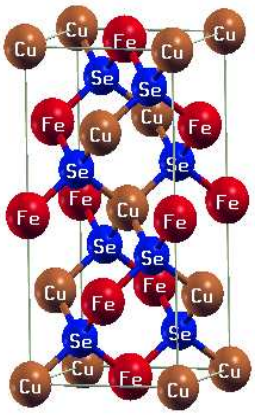

Figure 2: Unit cell of $CuFeSe_2$

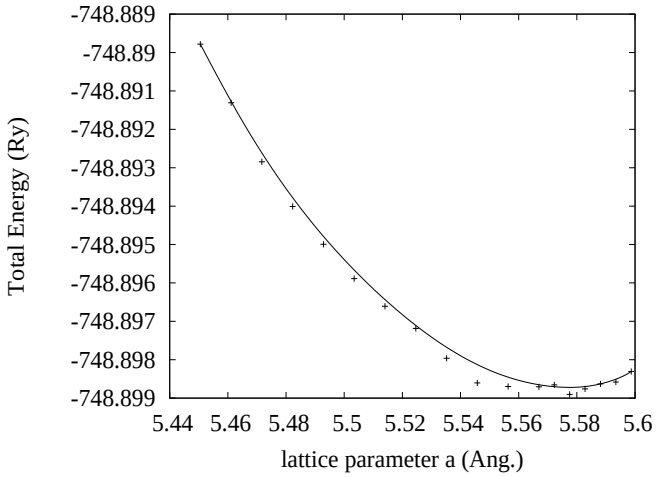

Figure 3: Total energy vs Lattice parameter'a' for $CuFeSe_2$

The structural parameters like lattice parameters, tetragonal distortion and anion displacement parameters are calculated using energy minimization procedure. Figure 3 and 4 show the total energy vs lattice parameter 'a' and total energy vs lattice parameter 'c' curve respectively. From these curves

Table 1: Structural parameters of $CuFeSe_2$. Numbers in square bracket represent reference.

	a(Å)	c (Å)	η	u_x	u_y	u_z
This work	5.578	11.153	0.999	0.252	0.249	0.124
Expt. work	5.50[9],5.53[10] 5.530[11],5.539[12]	11.00[9],11.05[10], 11.049[11],11.060[12]	1.0[12]			

the value of 'a' is found to be 5.578 Å and the value of 'c' is found to be 11.153 Å. The details of calculated structural parameters are given in Table 1. Table 2 shows the calculated bond lengths of the system.

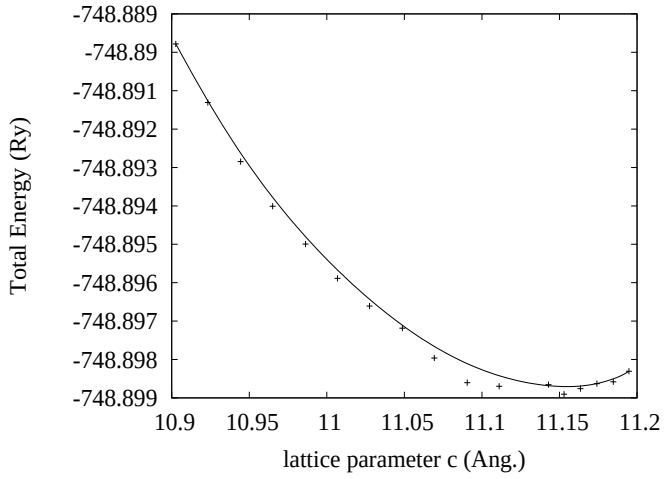

Figure 4: Total energy vs Lattice parameter'c' for $CuFeSe_2$

Figure 5 shows the band structure of $CuFeSe_2$. From this it is clear that $CuFeSe_2$ is a direct band gap semiconductor. Figure 6 shows the total density of states. From this figure it is clear that $CuFeSe_2$ is a p-type

Table 2: Calculated Bond lengths and Bond angles of $CuFeSe_2$

Cu-Se(Å)	Fe-Se(Å)	Cu-Se-Fe(degree)	Cu-Se-Cu(degree)	Fe-Se-Fe(degree)
2.423	2.408	109.48	108.97	109.98

semiconductor. The band gap is found to be 0.44 eV which is over estimated compared to experimental value [3,5]. Figure 7 shows the spin resolved density of states which shows that the spin up and spin down components are not identical.

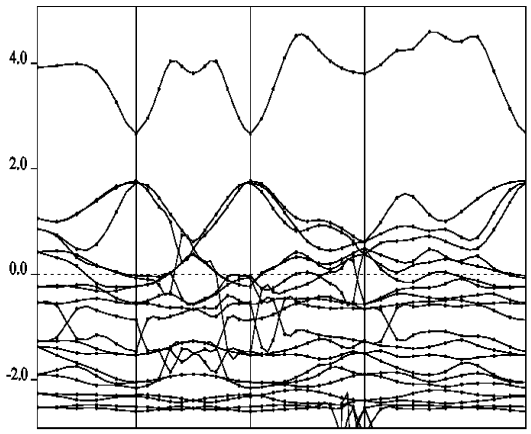

Figure 5: Band structure diagram of $CuFeSe_2$

Using linear response approach, U_{out} vs U_{in} curve is plotted. Taking the extrapolation of this curve, U_{scf} is found to be 3.11 eV.

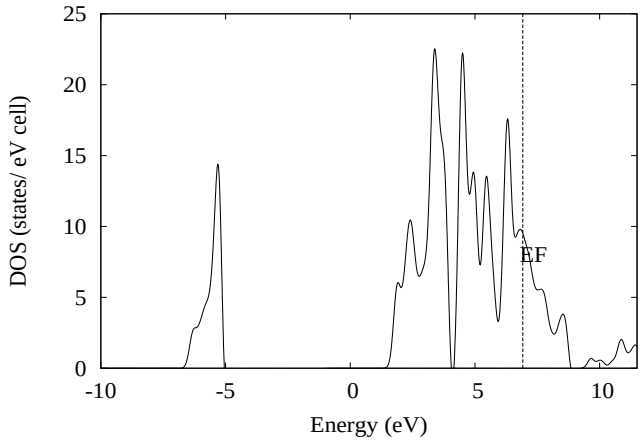

Figure 6: Total density of states of $CuFeSe_2$

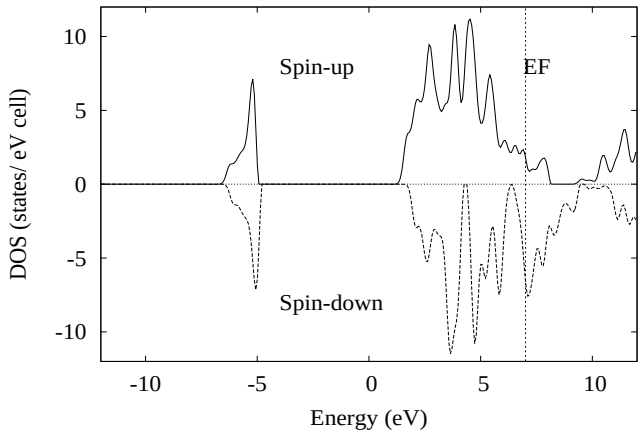

Figure 7: Spin resolved density of states for $CuFeSe_2$

4.2 $CdMnIn_2Te_4$

The plane wave cutoff energy (ecut) is found to be 25 Ry from figure 8. Unit cell of $CdMnIn_2Te_4$ is shown by figure 9. The positions of the various atoms in the tetragonal unit cell of $CdMnIn_2Te_4$ are: Cd(0,0,0), Mn(0,0.5,0.25), In_1(0,0,0.5), In_2(0,0.5,0.75) and Te(0.25,0.25,0.125).

Figure 10 shows the U_{out} vs U_{in} for $CdMnIn_2Te_4$. Extrapolating this

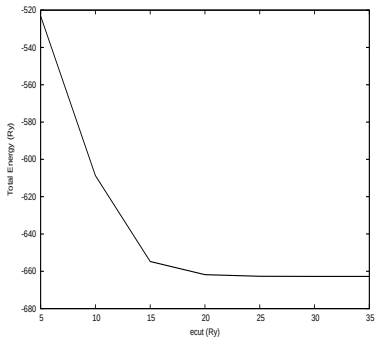

Figure 8: Total energy vs ecut

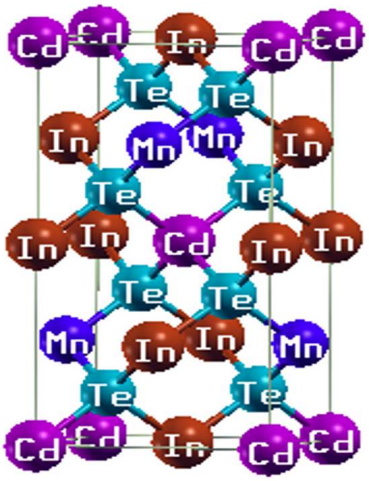

Figure 9: Unit cell of $CdMnIn_2Te_4$

curve U_{scf} is found to be 2.99eV. Using this Hubbard potential, a comparison is made on the structural and electronic properties of the $CdMnIn_2Te_4$.

Figure 11 shows the total energy vs lattice parameter 'a' for both without and with Hubbard correction. It shows that the lattice parameter'a' is found to be 6.702Å without application of U but with the Hubbard correction, it enhances to 6.782Å. Figure 12 shows the total energy vs lattice parameter 'c'

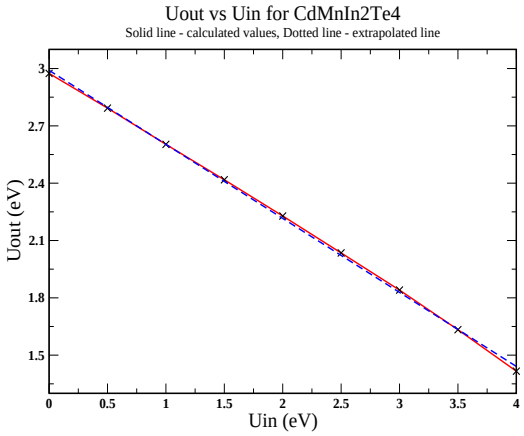

Figure 10: U_{out} vs U_{in} for $CdMnIn_2Te_4$

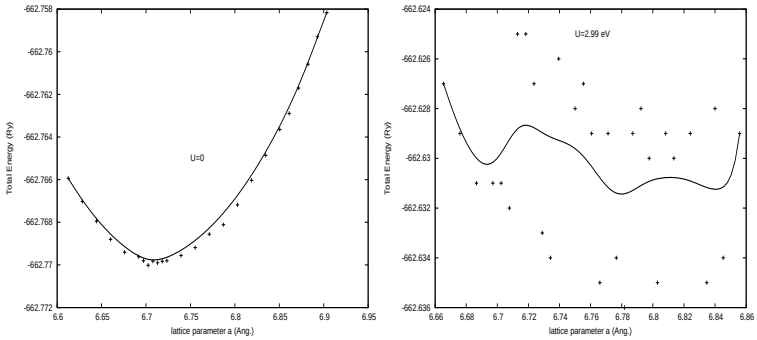

Figure 11: Total energy vs Lattice parameter 'a'for $CdMnIn_2Te_4$ without and with Hubbard Potential

without and with U for the system. Without Hubbard potential the lattice parameter 'c' is found to be 13.405Å but with Hubbard potential it increases to 13.561Å. The structural parameters are given in table 3. When Hubbard correction is applied, the value of lattice parameter 'a' and 'c' increases. Without application of Hubbard potential, η is found to be 1, which is the ideal condition but with the Hubbard potential η is reduced to 0.999 that is

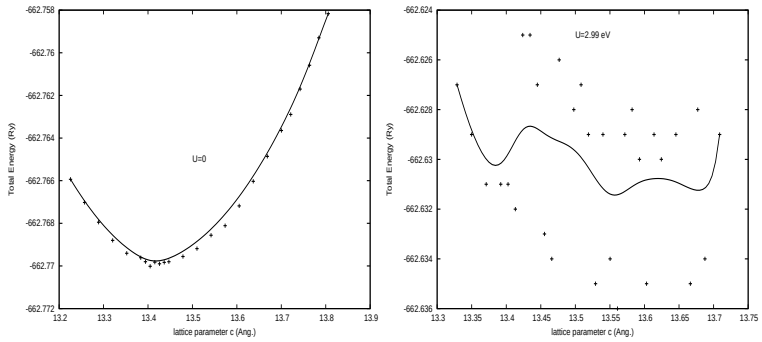

Figure 12: Total energy vs Lattice parameter 'c'for $CdMnIn_2Te_4$ without and with Hubbard Potential

Table 3: Structural parameters of $CdMnIn_2Te_4$.

	a(Å)	c (Å)	η	u_x	u_y	u_z
U=0	6.702	13.405	1.000	0.240	0.254	0.127
U=2.99	6.782	13.561	0.999	0.236	0.255	0.127

it no longer remains ideal. u_x, u_y, u_z are calculated, which shows that the system undergo anion displacement.

The calculated bond lengths and bond angles are given in table 4 and table 5 respectively. Table 4 shows that bond lengths increases when we give

Table 4: Bond lengths of $CdMnIn_2Te_4$.

	Cd-Te(Å)	Mn-Te(Å)	In_1-Te(Å)	In_2-Te(Å)
U=0	2.8995	2.8309	2.9422	2.9429
U=2.99	2.9289	2.8541	3.0036	3.0056

Table 5: Bond angles of $CdMnIn_2Te_4$.

	Mn-Te-Cd(degree)	Mn-Te-In(degree)	Cd-Te-In(degree)
U=0	111.643	110.395	108.495
U=2.99	112.623	110.382	108.352

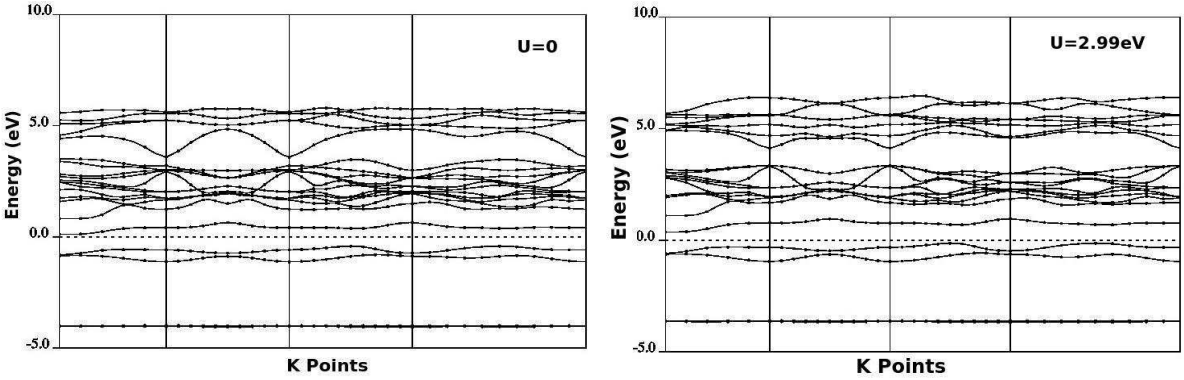

Figure 13: Band structure diagram for $CdMnIn_2Te_4$ for without and with Hubbard potential

Hubbard correction to the system.

The band structure for $CdMnIn_2Te_4$ is shown in figure 13 for both without and with Hubbard U. It shows $CdMnIn_2Te_4$ is a direct band gap semiconductor. An increase in band gap is observed in figure 13 from U=0 to U=2.99eV. That enhancement is calculated from total DOS plot.

Total density of states for without and with U is given in figure 14. It is clear that $CdMnIn_2Te_4$ is a n-type semiconductor for both the cases. The band gap is found to be 0.39 eV without U and with U it enhances to

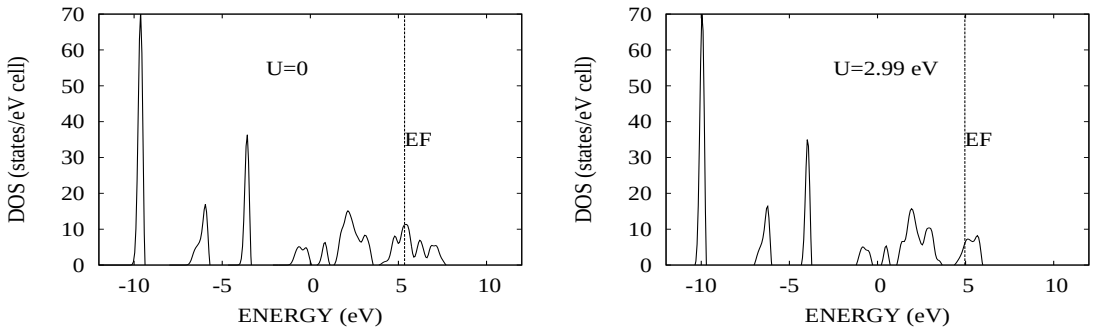

Figure 14: Total density of states for $CdMnIn_2Te_4$ both without and with Hubbard Potential

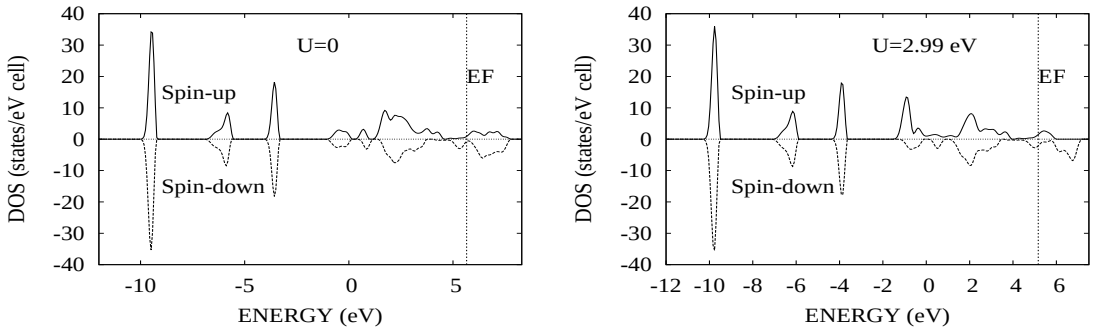

Figure 15: Spin resolved density of states for $CdMnIn_2Te_4$ both without and with Hubbard Potential

0.66eV. Figure 15 shows the spin resolved density of states for both without and with U for the system $CdMnIn_2Te_4$ and show that spin up and spin down components are not identical.

5 Conclusion

Structural and electronic properties of $CuFeSe_2$ and $CdMnIn_2Te_4$ are carried out using density functional theory, plane wave method and atomic pseudopotential included in quantum ESPRESSO. The Hubbard potential for $CuFeSe_2$ and $CdMnIn_2Te_4$ are found to be 3.11eV and 2.99eV respectively. The lattice parameters are found to be a=5.58Å, c=11.15Å for $CuFeSe_2$. For $CdMnIn_2Te_4$ the lattice parameters a and c are found to be 6.702Å and 13.405Å respectively. But with the application of Hubbard potential these values enhance to 6.782Å and 13.561Å respectively. The tetragonal distortion and anion displacement parameters are also calculated. Bond length and bond angles of $CuFeSe_2$ and $CdMnIn_2Te_4$ are calculated using Xcrysden. $CuFeSe_2$ is a p-type semiconductor but $CdMnIn_2Te_4$ is a n-type semiconductor. From the band structure diagram it is found that both $CuFeSe_2$ and $CdMnIn_2Te_4$ are direct band gap semiconductors. The band gap is found to be 0.44eV for $CuFeSe_2$ and for $CdMnIn_2Te_4$ it is found to be 0.39eV and 0.66eV for U=0 and U=2.99eV respectively. The spin up and spin down components are not identical.

6 References

1. *Mishra S. et.al.*,1. Effect of p-d hybridization and structural distortion on the electronic properties of $AgAlM_2$ (M = S, Se, Te) chacopyrite semiconductors, Solid State Communication, **151** (2011) 523-528.

2. Cu.pbe-d-rrkjus.UPF, Fe.pbe-sp-van.UPF and Se.pbe-van.UPF, Cd.pbe-n-van.UPF, Mn.pbe-sp-van.UPF, In.pbe-d-rrkjus.UPF and Te.pbe-rrkj.UPF from http://quantum-espresso.org.

3. *Giannozzi P. et. al.*, QUANTUM ESPRESSO: a modular and open source software project for quantum simulations of materials, Journal of Physics: Condensed Matter, **21** (2009) 395502.

4. *Kokalj A*, Computer graphics and graphical user interfaces as tools in simulations of matter at the atomic scale, Computational Material Science, **28** (2003) 155.

5. *Cococciono M. et.al.*, Linear response approach to the calculation of the effective interaction parameters in the LDA+U method, Phys Rev B **71** (2005) 035105.

6. *Kulik H.J. et.al.*, Density Functional Theory in transition metal chemistry: a self consistent Hubbard U approach, Phys Rev Lett **97** (2006) 103001.

7. *Hammdadou N. et.al.*, Fabrication of n and p type doped cuFeSe2 thin films achieved by selenization of metal precursor, Journal of Physics D:Apllied Physics, **39** (2006).

8. *Lee P.C. et.al.*, Cross plane seeback coefficient and thermal conductivity of $CuFeSe_2$ thin film, AIP Conference proceedings C: Measurement and characterization, **1449** (2011) 405-408.

9. *Najafov A.I. et.al.*, Growth technology and X-ray investigation results of $CuFeSe_2$ crystal modifications , Journal of Physics and Chemistry of solids, **64** (2003) 18731875 .

10. *KueiHsu-Yu et.al.*, One pot synthesis of $CuFeSe_2$ cubid nanoparticles, Materials Research Bulletin, **46** (2011) 2117-2119.

11. *Delgado J.M. et.al.*, The crystal structure of Copper Iron Selenide $CuFeSe_2$, Materials Research Bulletin,**27** (1992) 367-373.

12. *Lamazares J. et.al.*, Magnetic susceptibility, transport and Mossbauer measurements in $CuFeSe_2$, Hyperfine Interactions, *67*(1991) 517-522.

13. *Polubotko A.M. et.al.*, Ferron type of conductivity in metal $CuFeSe_2$, arXiv:1101.4904v2 [cond-mat.mtri-sci] (2011).

14. *Jie Wanqi .et.al.*, Crystal growth and characterizations of diluted mag-

netic semiconductor $Mn_xCd_{1-x}In_2Te_4$, Material science in semiconductor processing **8** (2005) 564-567.

15. *Chang Yongqin et.al.*, Composition distribution in the $Mn_xCd_{1-x}In_2Te_4$ ingot grown by ACRT-B method, J.Mater.Sci.Technol., **19(06)** (2003) 610-612.

16. *Chang Yongqin .et.al.*, Phase formation and physical properties of $Mn_xCd_{1-x}In_2Te_4$ ingots grown by Bridgman method, Journal of inorganic materials, **18(2)** (2003) 275-282.

17. *Palacio F. et.al.*, Magnetic characterization of the spin glass phase in $Mn_xCd_{1-x}In_2Te_4$ solid solutions, Materials science forum, **182-184** (1995) 459-462.